SPATIOTEMPORAL PATTERNS OF ENSO-PRECIPITATION RELATIONSHIPS IN THE TROPICAL ANDES OF SOUTHERN PERU AND BOLIVIA

A Thesis
by
JOSEPH ANTHONY JONAITIS

Submitted to the Graduate School
at Appalachian State University
in partial fulfillment of the requirements for the degree of
MASTER OF ARTS

December 2018
Department of Geography and Planning

SPATIOTEMPORAL PATTERNS OF ENSO-PRECIPITATION RELATIONSHIPS IN THE TROPICAL ANDES OF SOUTHERN PERU AND BOLIVIA

A Thesis
by
JOSEPH ANTHONY JONAITIS
December 2018

APPROVED BY:

L. Baker Perry, Ph.D.
Chairperson, Thesis Committee

Anton Seimon, Ph.D.
Member, Thesis Committee

Peter T. Soulé, Ph.D.
Member, Thesis Committee

Christopher Thaxton, Ph.D.
Member, Thesis Committee

Kathleen Schroeder, Ph.D.
Chairperson, Department of Geography and Planning

Mike McKenzie, Ph.D.
Dean, Cratis D. Williams School of Graduate Studies

Abstract

SPATIOTEMPORAL PATTERNS OF ENSO-PRECIPITATION RELATIONSHIPS IN THE TROPICAL ANDES OF SOUTHERN PERU AND BOLIVIA

Joseph Jonaitis
B.S., Michigan State University
M.A., Appalachian State University

Chairperson: L. Baker Perry, Ph.D.

Precipitation is vital in the outer tropical Andes, regulating freshwater availability, flooding, glacier mass balance, and droughts. Precipitation in the region, however, is highly seasonal and exhibits considerable interannual variability. The primary driver in interannual variability is the El Niño Southern Oscillation (ENSO), with most investigations reporting that the El Niño (La Niña) results in negative (positive) precipitation anomalies across the region. Recent investigations, however, have identified substantial spatiotemporal differences in ENSO-precipitation relationships. Motivated by the dissimilarity of these findings, this study examines a carefully selected dataset (≥ 90% completeness) of ground-based precipitation observations from 75 high-elevation (≥ 2,500 m asl) meteorological stations in the tropical Andes of southern Peru and Bolivia to identify distinct groups and associated variability in precipitation characteristics (e.g., total seasonal precipitation, wet season onset, and wet season length). Using no spatial constraints, the K-Means algorithm optimally grouped stations into five easily identifiable groups. Groups 3, 4, and 5 farthest from the Amazon basin had significant positive (negative) precipitation anomalies ($p < .05$) during La

Niña (El Niño), aligning with the traditional view of ENSO-precipitation relationships while Groups 1 and 2 closest to the Amazon had opposite relationships. Additionally, though studies have reported delays in the wet season, years characterized by El Niño had an earlier wet season onset in all five groups. These findings may aid in improving seasonal climate prediction and managing water resources, and could also allow for improved interpretation of tropical Andean ice cores.

Acknowledgments

The completion of this master's thesis is the culmination of thousands of hours of support given to me by numerous individuals and organizations throughout my life. My parents, grandparents, and extended family fostered my continuous desire to learn, my strong faith, and a commitment to serving others. What I learned and received early on from them has been a bedrock in my life. Numerous teachers in high school and at the undergraduate level dedicated their time to challenging and guiding me during my academic career. Their continuous efforts along with multiple opportunities to volunteer, work, and study abroad enhanced my academic learning and personal growth and positively impacted the direction of my life.

Ten years after I graduated from Michigan State University, Dr. L. Baker Perry believed in my potential and offered me a position on his research team in conjunction with earning a master's degree in Geography at Appalachian State University. Through his NSF Grant AGS-1347179 (CAREER: Multiscale Investigations of Tropical Andean Precipitation), he not only funded the majority of my tuition, but also paid for a research expedition in Peru, scientific conferences in Peru and New Orleans, and snow measurement school in Colorado. His generosity is only surpassed by his work ethic, a trait that serves as an inspiring example for his whole department. Dr. Anton Seimon also was instrumental in my career at Appalachian, providing thoughtful and well-communicated critiques and advice. Together, they, along with my other thesis committee members, Dr. Christopher Thaxton and

Dr. Peter Soulé, patiently guided me through the struggles, challenges, and victories I experienced while completing my thesis and master's degree. Though not on my committee, Dr. Johnathan Sugg and Montana Eck provided critical advice that I implemented while writing this paper. Tania Ita Vargas also was a wealth of knowledge and huge help in securing precipitation observations from Peru and determining the best method for finding wet season onset. Additionally, the men and women of the weather service in Peru (SENAMHI Peru), the weather service in Bolivia (SENAMHI Bolivia), and governmental organizations such as Earth System Research Laboratory of the U.S. National Oceanic and Atmospheric Administration, provided necessary climate data. Without their work, I would not have been able to complete my thesis.

Appalachian State University, Boone, and the surrounding communities fully welcomed our family. Having never been to North Carolina before, my wife and I knew no one. From our neighbors, Steve and Cindy Blind, to our church community at St. Elizabeth Church and Church of the Epiphany, we were received with open arms and hearts. My professors at Appalachian were incredibly helpful during my formation here; they always had an open door and treated us graduate students with respect. Steven Vacendak and the Office of Student Research also provided a scholarship and grant that funded part of my tuition and expenses to present my research, respectively. My classmates were essential in talking through numerous challenges and helping me balance long study nights with fun events like Friendsgiving and tailgating. My classmates even threw my wife and me a touching baby shower, even as busy and low on cash as we graduate students are.

Finally, my wife Jenna has been an incredible motivation and support in my life. She agreed and supported us moving to North Carolina so that I could pursue my master's degree.

I was very lucky that her career as a writer supported our family from anywhere. She has always believed in me and counseled me even when my doubts were great and my obstacles seemed insurmountable. She constantly reminds me through her words and actions of the beauty and bigger purpose in life, and she is a source of so much laughter and light for me. The greatest gift she gave while in Boone, though, was our first-born child.

For all these people, opportunities, and organizations, and for God for putting them all in my life, I am incredibly thankful. I feel so grateful for so many blessings and know that I would not be where I am right now without them.

Dedication

I dedicate this thesis to my loving and beautiful wife Jenna Rose, our baby John Casimir, and any other future children with which God may bless our family.

Table of Contents

List of Tables

List of Figures

Foreword

The main body of this thesis is formatted to the guidelines for manuscript submission to the *International Journal of Climatology*, an official journal of the Royal Meteorological Society.

Introduction

Known for being the longest continental mountain range in the world and running more than 7,000 km along the western edge of South America, the Andes Mountains are home to some of the world's most diverse mountainous environments. These mountains are also home to 99% of the all the tropical glaciers in the world, with Peru and Bolivia claiming 71% and 20%, respectively (Francou and Vincent 2007, Rabatel et al. 2013). Glaciers provide freshwater to cities such as La Paz, Bolivia, and Lima, Peru, and store hundreds to thousands of years of climatic paleoindicators (Thompson et al. 1986, Ramirez et al. 2003, Haines et al. 2016). Present day Andean glacier mass balance is highly negative, however, with annual losses of 0.76 m water equivalent since 1974, nearly four times faster than the prior decade (Rabatel et. al 2013). Amplified warming in this region could mean temperature increases of 5°-6°C under the IPCC A2 emissions scenario by the end of this century (Urrutia and Vuille 2009) with all glaciers below 5,400 m asl (asl is omitted hereafter), constituting approximately 50% of tropical glaciers in area, disappearing (Soruco et al. 2009).

Primary mechanisms for glacial loss include increasing temperatures (Bradley et al. 2006, Ramirez et al. 2001), variable precipitation, and possible changes in cloud cover (Francou et al. 2003, Favier et al. 2004). Glacier loss and precipitation are closely linked, in that solid precipitation primarily regulates the absorption and reflection of incoming solar radiation on the glaciers (Rabatel et al. 2013). Glaciers in southern Peru and Bolivia face increased ablation when fresh snow does not fall, especially during clear days at the end of the dry season when the glaciers have their lowest albedo (Ribstein et al. 1995, Francou et al. 2003, Sicart et al. 2011).

Although glacier mass balance is influenced by precipitation (Favier et al. 2004), there are challenges to studying precipitation in the outer tropical Andes. The region has spatially complex precipitation patterns (Aalto et al. 2003, Ronchail and Gallaire 2006), sparse precipitation observations, and diverse terrain ranging from below 2,500 m asl to 6,542 m.

El Niño-Southern Oscillation (ENSO) determines the majority of inter-annual precipitation variability in the outer tropical Andes (Francou and Pizarro 1985, Vuille et al. 2000, Garreaud and Aceituno 2001). Previous investigations (Garreaud and Aceituno 2001, Ronchail and Gallaire 2006, Rabatel et al. 2013, Vuille et al. 2000) report that the warm phase of ENSO (El Niño) is typically associated with negative annual precipitation anomalies, whereas the cold phase of ENSO (La Niña) is typically associated with positive annual precipitation anomalies. More recent studies that attempt to characterize the ENSO-precipitation relationships, however, challenge the traditional view of ENSO-precipitation relationships in the region (Perry et al. 2014, Perry et al. 2017, Sulca et al. 2017).

Due to the inconclusiveness of the scientific findings and the need for accurate climatic predictions, (Perry et al. 2014, Perry et al. 2017, Sulca et al. 2017, Vuille et al. 2000), I decided to investigate ENSO-precipitation relationships in the Andean Mountains of southern Peru and Bolivia. Because satellite-based datasets such as the Tropical Rain Measuring Mission (TRMM) underestimate precipitation in the tropical Andes by up to 35-40% (Espinoza et al. 2015, Chavez and Takahashi 2017) and models such as the Weather Research and Forecasting model, version 3.4.1 (Skamarock et al. 2008) overestimate precipitation in the region (Junquas et al. 2018), I used daily ground-based precipitation data recorded by rain gauge networks. Furthermore, this study only used stations from selected high elevation sites (≥ 2,500 m) in the study region with near complete (≥ 90%) precipitation records from 1972-2016 (Fig. 1) to ensure a representative data set. Using these observations, I computed precipitation characteristics for each station, such as total wet season precipitation, wet season onset, and number of wet days for each hydrological year. To investigate the intraregional variability of precipitation (e.g. Eck et al. 2018), the study region was classified into five distinct groups through a K-means test, which determined the optimal number of groups and maximized within group precipitation characteristic similarities and outside group differences in precipitation characteristics. All groups were elongated with their axis aligned parallel to the Andes with Groups 1 and 2 in the north and east and Groups 3, 4, and 5 in the south and west closest to the Pacific Ocean. Groups The Kruskal-Wallis H test, suitable for three or more groups of non-parametric data, and a post-hoc test for the Kruskal-Wallis H (Kruskal and Wallis 1952) tested for significant differences among ENSO phases in each of the groups.

This paper has improved the understanding of ENSO-precipitation relationships that shape the prediction of tropical Andean precipitation and interpretation of tropical Andean ice cores across the Northern Altiplano. Though some studies suggested wet season onset is delayed during El Niño when compared with ENSO Neutral or La Niña years, wet season onset is earliest during El Niño years (n = 17 events) in all five station groups. La Niña years (n = 10 events) had the latest onset in four of the five groups. Furthermore, a distinct east-west ENSO-precipitation dipole was uncovered. While the western groups (Groups 3, 4, and 5) largely followed the traditional understanding of ENSO-precipitation relationships, eastern groups (Groups 1 and 2), which include important ice core sites such as the Quelccaya Icecap, demonstrated opposite relationships. These results will provide relevant information to better understand the distinct influences of past and future ENSO events on the spatially variable characteristics of precipitation in the region. Such understanding will not only aid in managing water resources in this area, which primarily receives precipitation from November to March, but may inform the interpretation of ice core records and other paleoclimatic archives within this study region.

Spatiotemporal Patterns of ENSO-Precipitation Relationships in the Tropical Andes of Southern Peru and Bolivia

Joseph A. Jonaitis[1], L. Baker Perry[1], Anton Seimon[1,2], Peter T. Soulé[1], Christopher Thaxton[3], Marcos F. Andrade-Flores[4], Maxwell Rado[5], Tania Ita Vargas[1], Laura Ticona[4]

[1]Department of Geography and Planning, Appalachian State University, USA
[2]Climate Change Institute, University of Maine, USA
[3]Department of Physics and Astronomy, Appalachian State University, USA
[4]Laboratorio de Física de la Atmosfera, Instituto de Investigaciones Físicas, Universidad Mayor de San Andrés, Bolivia
[5]Observatorio Meteorológico, Universidad Nacional de San Antonio Abád del Cusco, Perú

Abstract

Precipitation is vital in the outer tropical Andes, regulating freshwater availability, flooding, glacier mass balance, and droughts. Precipitation in the region, however, is highly seasonal and exhibits considerable interannual variability. The primary driver in interannual variability is the El Niño Southern Oscillation (ENSO), with most investigations reporting that the El Niño (La Niña) results in negative (positive) precipitation anomalies across the region. Recent investigations, however, have identified substantial spatiotemporal differences in ENSO-precipitation relationships. Motivated by the dissimilarity of these findings, this study examines a carefully selected dataset (≥ 90% completeness) of ground-based precipitation observations from 75 high-elevation (≥ 2,500 m asl) meteorological stations in the tropical Andes of southern Peru and Bolivia to identify distinct groups and associated variability in precipitation characteristics (e.g., total seasonal precipitation, wet season onset, and wet season length). Using no spatial constraints, the K-Means algorithm optimally grouped stations into five easily identifiable groups. Groups 3, 4, and 5 farthest from the Amazon basin had significant positive (negative) precipitation anomalies ($p < .05$) during La Niña (El Niño), aligning with the traditional view of ENSO-precipitation relationships while Groups 1 and 2 closest to the Amazon had opposite relationships. Additionally, though studies have reported delays in the wet season, years characterized by El Niño had an earlier wet season onset in all five groups. These findings may aid in improving seasonal climate prediction and managing water resources, and could also allow for improved interpretation of tropical Andean ice cores.

1. Introduction

The Andes Mountains, the longest continental mountain range in the world, contain some of the world's most diverse habitats and 99% of all the tropical glaciers in the world, with Peru and Bolivia claiming 71% and 20%, respectively (Francou and Vincent 2007, Rabatel et al. 2013). Glaciers store thousands of years of climate records (Thompson et al. 1986, Ramirez et al. 2003, Haines et al. 2016) and help regulate regional natural hazards such as landslides, floods, droughts, and water shortages in this region (Anderson et al. 2017, Vuille et al. 2017). Andean glacier mass balance is highly negative at present (Rabatel et. al 2013), however, and predicted amplified warming of 5°-6°C by the end of the century (Urrutia and Vuille 2009) in this region could mean the disappearance of all glaciers below 5,400 m asl (asl is omitted hereafter), approximately 50% of glaciers in area (Soruco et al. 2009).

Primary mechanisms for glacial loss in the outer tropical Andes of southern Peru and Bolivia, a region between 12-18 °S which includes part of the Altiplano, include increasing temperatures (Bradley et al. 2006, Ramirez et al. 2001), variable precipitation, and possible reduction in cloud cover (Francou et al. 2003, Favier et al. 2004). Glacier loss and precipitation are closely linked, although there are numerous challenges to studying precipitation including spatially complex precipitation patterns (Aalto et al. 2003, Ronchail and Gallaire 2006), scarce observations, and high topographic relief ranging from below 2500 m asl to 6,542 m asl. The El Niño-Southern Oscillation (ENSO) determines the majority of inter-annual precipitation variability in the outer tropical Andes (Francou and Pizarro 1985, Vuille et al. 2000, Garreaud and Aceituno 2001) with initial research (e.g. Vuille et al. 2000, Garreaud and Aceituno 2001, Ronchail and Gallaire 2006, Rabatel et al.

2013) indicating positive and negative precipitation anomalies occurring during the warm phase (El Niño) and cold phase (La Niña), respectively. Precipitation responses to ENSO phases have been found to reverse over time near the study area (Aalto et al. 2003) and vary adjacent to the study area (Ronchail and Gallaire 2006) (Fig. 1). The most recent studies (Perry et al. 2014, Perry et al. 2017, Sulca et al. 2017) characterizing the ENSO-precipitation relationships in the region, however, have challenged this initial view with ENSO phases associated with opposing precipitation anomalies in some parts of the study area.

To resolve the differences among these studies, the present study investigates the subregional variability of ENSO-precipitation relationships in the Andes of southern Peru and Bolivia. In order to identify the ENSO-precipitation relationships in this intermontane region, this investigation examines gauge-based precipitation data from selected high elevation sites (≥ 2500 m) that have near complete (≥ 90%) precipitation records over a 45-year period (Fig. 1). The study region is divided into optimally selected groups in order to investigate intraregional variability of precipitation (e.g., Eck et al. 2018). The distinct patterns identified by these new analyses help to resolve disparities among previous studies and may provide critical information to scientists and local stakeholders to improve scientific understanding of ENSO-precipitation relationships in the outer tropical Andes.

2. Background and Literature Synthesis

Precipitation in the outer tropical Andes has distinct seasons, with a single wet season typically extending from October to March (Perry et al. 2017). Seasonal precipitation totals increase over the study region from the southwest to the northeast, and over 50% of precipitation occurs during the austral summer from December to February (Garreaud and

Aceituno 2001, Perry et al. 2014). The wet season occurs when latent heating from Amazon monsoonal convection associates with the formation of the Bolivian High and Chaco Low at upper and lower levels of the atmosphere, respectively (Figueroa et al. 1995, Rodwell and Hoskins 2001, Seluchi et al. 2003). The northern branch of the Bolivian High is associated with upper-level (300 - 200 hPa) easterly winds, which are correlated with mid-level moisture transport from the Amazon and convection in the Andes Garreaud (1999). The wet season in the region is characterized by northerly and easterly flow at lower levels. Conversely, westerly winds at the lower levels with low specific humidity dominate the dry season, and are associated with a near complete dissipation of the Bolivian high (Vuille et al. 1998, Garreaud et al. 2003). In the intermontane region, pluvial periods lasting one to two weeks alternate with dry periods of equal length (Garreaud and Aceituno 2001, Guy et al., forthcoming, 2018). This episodic pattern is regionally coherent (Garreaud 2000, Perry et al. 2014) and likely linked with the South American Low Level Jet (SALLJ), which influences moisture provision from the Amazon lowlands to the Andes (Guy et al. forthcoming, 2018). At the diurnal time scales, precipitation in the outer tropical Andes occurs predominantly as convective events during the afternoon and longer-lasting stratiform events during the nighttime (Perry et al. 2014, Chavez and Takahashi 2017, Junquas et al. 2018).

Precipitation falling in the outer tropical Andes is controlled by moisture availability and its transport to the area (Garreaud 1999). The Amazon Basin is the source of about 95% of the moisture for precipitating events in the region, as inferred from backward air trajectories of precipitating events in Cusco and La Paz (Perry et al. 2014). Moisture transport is primarily light, around 1-3 m s^{-1} (Vimeux et al. 2005, Perry et al. 2014), is parallel with and enhanced by the SALLJ (Junquas et al. 2018), and originates from the west and north in southern Peru and east and north in Bolivia (Perry et al. 2014, Ronchail and Gallaire 2006). Though seemingly contradictory, northwesterly moist flow in southern Peru still advects moisture from the Amazon basin due to the area's unique geomorphology. Over the Bolivian Altiplano, precipitation decreases occur from east to west and north to south as moisture is uplifted while crossing the Andes (Ronchail and Gallaire 2006). Valleys which cut across the Andes and orient with the SALLJ from northwest to southeast channel the moisture to the region (Junquas et al. 2018).

Contributing to the majority of inter-annual precipitation variability in the region (Francou and Pizarro 1985, Vuille et al. 2000, Garreaud and Aceituno 2001), ENSO is a complex teleconnection pattern with distinct signals throughout the world. Its warm phases (El Niño) and cold phases (La Niña) typically last nine to twelve months and occur on average every four years (Trenberth 1997). Both phases normally begin to develop from June to August and reach their peak strength between December and April of the following year (Philander 1983, Trenberth 1997), coinciding with the wet season peak within the study region.

Like ENSO, the Pacific Decadal Oscillation (PDO) also associates with SST variability in the Pacific. The SST changes during the warm PDO phase associate with precipitation deficits in tropical South America (Mantua and Hare 2002). A climatic regime shift identified with the PDO and the North Pacific occurred during the northern hemisphere winter of 1976-77 and associated with widespread warming over the tropical Pacific similar to El Niño (Graham 1994, Nitta and Yamada 1989).

Many investigations (e.g., Aceituno 1988, Vuille 1999, Vuille et al. 2000, Garreaud and Aceituno 2001, Ronchail and Gallaire 2006, Rabatel et al. 2013) using a variety of methods have found that El Niño correlates with negative precipitation anomalies and La Niña correlates with positive precipitation anomalies in the outer tropical Andes. Knüsel et al. (2005) analyzed precipitation data, ENSO phase, and dust-related ions deposited between 1887 and 1999 in an ice core from Nevado Illimani (~6,300 m) in Bolivia. Increased dust correlated with decreased precipitation and El Niño; decreased dust correlated with increased precipitation and La Niña. Since glacial mass balance depends on the inter-annual variability of precipitation (Favier et al. 2004), Veettil et al. (2016) concluded that rises in snowline altitude (SLA) corresponded with decreases in precipitation. Selected glaciers in the Cordillera Occidental and the Cordillera Oriental tended to have higher SLAs during El Niño and lower SLAs during La Niña (Veettil et al. 2016). Furthermore, when the warm phase of PDO and El Niño and the cold phase of PDO and La Niña aligned, the effects of El Niño and La Niña were stronger on SLA. Increased glacial runoff from the Zongo glacier 30 km north of La Paz was also associated with El Niño when compared with runoff during ENSO Neutral (i.e. neither El Niño or La Niña) years (Ribstein et al. 1995). The amount of precipitation attributed to the runoff, however, actually decreased when compared with ENSO Neutral phase years, suggesting negative precipitation anomalies during El Niño when compared with ENSO Neutral phase years (Ribstein et al. 1995).

Recent attempts to characterize ENSO-precipitation relationships using ground-based precipitation data in the outer tropical Andes show conflicting results. Perry et al. (2014) found that portions of the Cordillera Oriental near Cusco had negative precipitation anomalies during the 2007-08 La Niña and positive precipitation anomalies during the subsequent 2009-10 El Niño (Perry et al. 2014). In an additional study (Perry et al. 2017), La Paz experienced negative precipitation anomalies during both phases of ENSO from 1979-

2009. Cusco, on the other hand experienced positive precipitation anomalies during El Niño and negative anomalies during La Niña from 1963-2009 (Perry et al. 2014, Perry et al. 2017).

Further illustrating the complexity of the effect of ENSO on the region, Aalto et al. (2003) analyzed sediment cores near rivers in the eastern side of the Cordillera Oriental of northern Bolivia using lead isotopes to determine individual sediment events. The authors found that rapidly rising floods occurred more frequently during La Niña. More importantly, they noted that in part of the floodplain, the response to ENSO flipped in the early 1970s—such that rainfall was actually lower during La Niña and sometimes higher during El Niño (Aalto et al. 2003). In an additional study (Ronchail and Gallaire 2006) that examined precipitation observations, ENSO demonstrated distinct relationships on opposite sides of the Cordillera Oriental of northern Bolivia. While the western side of the cordillera and the Altiplano of Bolivia recorded negative precipitation anomalies during El Niño and positive precipitation anomalies during La Niña, the opposite precipitation anomalies occurred on the eastern side of the cordillera (Ronchail and Gallaire 2006). Location and timing seemed to play a crucial role on how the ENSO-precipitation relationship is expressed, even within regions of Bolivia.

The primary research question we address in this study is: how do precipitation and its characteristics vary across space and through time as a function of ENSO phase over the study area? The analyses are based on daily precipitation observations from 75 high-elevation sites (≥ 2500m) in the Andes of southern Peru and Bolivia with near complete precipitation records (≥90%) over a 45-year period. This work is motivated by the identified need to improve scientific understanding of ENSO-precipitation relationships in space and time, and the desire to provide better guidance to stakeholders in the region who need to plan for a changing climate and to scientists interpreting ice cores from glaciers in the region.

3. Data and Methods

Study Area and Datasets

The Peruvian National Meteorology and Hydrology Service (SENAMHI), Bolivian SENAMHI, and the project Data on Climate and Extreme Weather for the Central Andes (DECADE) (Andrade et al. 2018, Hunziker et al. 2018) provided daily precipitation observations from stations between 12.5°S and 18°S in southern Peru and Bolivia (Table 1). The precipitation observations, which originated from 533 Peruvian SENAMHI and 241 Bolivian SENAMHI manual and automatic stations, spanned from 1931 to the present and from 1917 to the present, respectively. In order to focus on the north central Altiplano and its bordering areas, the study region only included stations ≥ 2500 m asl. This study only used stations with 90% completeness in their data set, surpassing the minimum recommended completeness for climate normals (80%) (WMO 2011). The analysis extends from 1 July 1972 – 30 June 2017 (hereafter referred as hydrological years 1972-2016 or simply 1972-2016) because the period includes the greatest number of stations (76) at 90% completeness over the longest time series including multiple El Niño and La Niña events.

Computation of Precipitation Characteristics

The daily precipitation observations provided the foundation for determining a set of climatological characteristics, namely: total hydrological year (1 July – 30 June) precipitation, total wet season precipitation, wet season onset, dry season onset, wet season length, peak wet season date, number of wet days, and number of very wet days for each observation site. Liebmann et al. (2007) detailed the method for computing the wet and dry season onset used to derive the wet season length and total wet season precipitation. The average wet season onset for the entire period (1972-2016) was determined by computing three values: 1) the daily mean precipitation over the entire period, 2) the daily difference between the daily mean precipitation and the overall mean for the entire period, and 3) the cumulative sum of the daily difference, starting on 1 July. For example, all precipitation records from 1 July through the entire period were averaged to obtain the daily mean precipitation for that date. The daily mean amount was subtracted from the overall mean precipitation from 1972-2016 to compute the daily difference. Finally, the difference found on 1 July was added to the difference found on 2 July to find the cumulative sum on 2 July. Because very little precipitation falls from July through October, the cumulative sum produces a negative slope during the same months. As the wet season approaches and mean daily precipitation begins to exceed mean precipitation for the period, the slope becomes positive. The day associated with the minimum in the cumulative sum denotes the wet season onset. Conversely, the day associated with the maximum in the cumulative sum when the overall mean precipitation begins to exceed the mean daily precipitation indicates the dry season onset. In addition, the peak wet season date corresponded to the maximum value of the slope of the cumulative sum. Prior to determining the peak and onset dates, a 14-day rolling mean for the cumulative sum was employed to smooth precipitation cycles. A station that recorded measurable precipitation (>0) during a calendar day signified one wet day. A very wet day was counted when a station recorded precipitation during a calendar day that was at or above the 95th percentile of all precipitation observations during the entire study period.

Grouping Analysis

The K-Means algorithm (Hartigan and Wong 1979), a grouping analysis tool in ESRI's ArcMap 10.4.1, grouped stations by their precipitation characteristics without employing spatial constraints. The tool constructed different groups by finding the starting stations that had the greatest differences in a characteristic and then grouping other stations with similar characteristics to those starting stations. The station characteristics used to group the stations included all of the aforementioned precipitation characteristics, geographical properties of the station such as latitude and elevation, and combinations of all of these characteristics. Multiple grouping analyses were performed, testing how well different station characteristics grouped stations. An R^2 value and a Calinski-Harabasz pseudo F-statistic (F) (Calinski and Harabasz 1974) assessed both the fitness of the precipitation characteristic(s) used and the groups developed. The closer an R^2 value was to 1.0, the better the precipitation characteristic was for discriminating among the stations in the groups produced. This study sought groups of stations with R^2 values over 0.95. Two to fifteen hypothetical groups were produced for each grouping analysis. Each set of groups produced an F that reflected within-group similarity and between-group difference. The optimal number of groups demonstrated the highest F value while also maintaining the lowest number of groups. When grouping stations by wet season onset, the algorithm consistently placed one station farthest to the north (Huancalpi, Huancavelica, Peru at 12.539°S and 75.237°W) in its own group since its wet season onset was twenty-four days earlier than the station with the next earliest wet season onset. For this reason, the station was not included in the dataset when grouping by wet season onset and was not included in subsequent analysis.

Identifying ENSO-Precipitation Relationships

The eight precipitation characteristics were computed for the overall study region and for each group during each hydrological year from 1972-2016. In addition to these characteristics, the coefficient of variation (CV) was computed for total wet season precipitation. Following Climate Prediction Center (2018) protocol for the Oceanic Niño Index, each hydrological year was categorized as an El Niño or La Niña year if five or more consecutive bi-monthly index values from the Multivariate ENSO Index (MEI) (Earth System Research Lab) were greater than 0.5 or less than -0.5, respectively (Table 1). Any years not identified as El Niño or La Niña were categorized as ENSO Neutral years. The Kruskal-Wallis H (Kruskal and Wallis 1952) test revealed if any ENSO phase exhibited significant differences in the precipitation characteristics. A post-hoc Kruskal-Wallis H test (Dunn 1964), which employed a Bonferroni correction for multiple tests (Bonferroni 1936), then completed a pairwise comparison of all ENSO phases to reveal which ENSO phase pairs had significant differences. Unless otherwise noted, all differences reported were significant at the 0.05 level. For further validation, the Spearman's rank-order correlation tested the strength and direction between various groupings of MEI values and the precipitation characteristics.

4. Results

Groups and their Precipitation Characteristics

Average wet season onset grouped the 75 stations in the study area most effectively (Fig. 1). The grouping analysis produced four and five station groups with R^2 values of 0.9702 and 0.9792, respectively. These two groupings represented the minimum number of station groups that produced R^2 values over 0.95. Groupings with more than five station groups were not considered even if they had R^2 values over 0.95. The F also had increased values when stations were divided into four or five groups when compared with fewer groups. Multiple iterations of the grouping analysis revealed that F values remained relatively constant when grouping stations into five groups but had substantial drops when grouping stations into four groups. Since grouping the stations into five sets produced a higher R^2 value and a consistently high F, the authors chose to group stations into five groups. Although the groups were largely spatially contiguous, large gaps in station data south and west of Cusco made delineation of geographic regions highly uncertain.

The five groups followed a NW – SE orientation, were numbered from 1-5, and ordered from earliest to latest wet season onset date (Fig. 2a). Group 1 incorporated the eastern Peruvian highlands, Quelccaya Ice Cap, and Cusco, while Group 2 incorporated most of Lake Titicaca, the northeastern Bolivian highlands, La Paz, and Nevado Chacaltaya. Median station elevation for Groups 1 and 2 were 3,903 and 3,840 m, respectively (Fig. 2b). Groups 3, 4, and 5 were in the western cordillera and highlands of Peru and Bolivia with a median station elevation of 3,872, 3,367, and 3,214 m, respectively. Groups 3, 4, and 5, which were closest to the Pacific coast, demonstrated the latest average wet season onsets (7, 15, and 29 December respectively), and Groups 1 and 2, closest to the Amazon Basin, had the earliest wet season onset (11 and 20 November respectively).

Precipitation was highest in Groups 1 and 2 with 569 and 516 mm average total precipitation during the wet season (Table 2) and 686 and 641 mm average total precipitation during the hydrological year, respectively (Fig. 2c). Groups 3, 4, and 5 followed regional patterns receiving 500, 398, and 219 mm on average during the wet season (Table 2) and 602, 462, and 240 mm on average during the hydrological year. The farther south and west the groups were from the Amazon Basin, the less seasonal and annual total precipitation the groups received. The CV, which was lowest and nearly identical in Groups 1 and 2, increased spatially to the south and west coast (Fig. 2d). Group 5 had the highest CV indicating that the greatest variability in seasonal precipitation occurred in the west closest to the Pacific coast. The frequency of wet days and very wet days followed precipitation totals; both were highest in groups nearest the Amazon lowlands in the east and lowest near the coast in the west (Figs. 2e and 2f).

Regional and Group Response to ENSO

The study region as a whole and as individual groups showed statistically significant differences between pairs of different ENSO phases. The overall study region experienced increased total wet season and hydrological year precipitation during ENSO Neutral years (66 and 74 mm more, respectively) compared with El Niño years (Table 2). Though not statistically significant, wet season onset occurred, on average, 11 days earlier during El Niño than during La Niña in the overall study region (Table 4). The dry season onset was also not statistically different among any ENSO phase for any of the groups or the study region as a whole. The average dry season onset occurred on 12 April within the overall study region and within seven days from that date among all ENSO phases in all the groups.

Groups 1 and 2 exhibited the most precipitation, wet days, and very days during El Niño years and the earliest wet season onset in ENSO Neutral years. Both saw an earlier wet season onset (20 and 27 days earlier, respectively) and longer wet season length ($p<0.1$ for Group 2 only) during hydrological years with El Niño than with La Niña. Group 1 also had 1.3 more very wet days during El Niño years than in La Niña years (Fig. 3 and Tables 4 and 5). For both Groups 1 and 2, ENSO Neutral years received the greatest total wet season precipitation (77 and 82 mm, respectively) ($p<0.1$) when compared with La Niña years (Figs. 4 and 5 and Table 2). Wet season onset occurred 16 days earlier on average in Group 2 during ENSO Neutral years in contrast with La Niña years (Table 5).

Groups 3, 4, and 5 also showed very similar precipitation characteristics in precipitation, number of wet days and wet season onset. All three groups received increased wet season precipitation (81, 135, and 133 mm more, respectively) during La Niña events when compared with El Niño events (Figs. 4 and 5 and Table 2). La Niña years also reported significantly increased total annual precipitation, more wet days, and more very wet days (1.5 and 1.5 days more, respectively) (Table 3) than El Niño years in Groups 4 and 5. ENSO Neutral years showed an increase of 94 mm in total wet season precipitation and 102 mm ($p < 0.1$) in total annual precipitation when compared with El Niño years in Groups 3 (Figs. 4 and 5 and Table 2). La Niña years also experienced positive wet season precipitation anomalies (78 mm) (Table 2) and positive annual precipitation anomalies (85 mm more) than ENSO Neutral years in Group 5.

Spearman's rank-order correlation validated and matched the significant differences found in precipitation characteristics between El Niño and La Niña years for the study region as a whole and for individual groups (Table 6). The January-February MEI value corresponded best with precipitation in Groups 3, 4, and 5 and the September-October MEI value corresponded best with wet season onset in Groups 1 and 2.

5. Discussion

Seasonal and Yearly Accumulation

Differences in positive and negative precipitation anomalies in the study region as a whole and within the individual groups showed similarity with the ENSO-precipitation relationships previously identified for the region. The overall study region received lower annual and wet season precipitation ($p < 0.1$) during El Niño years, consistent with previous studies (Aceituno 1988, Vuille 1999, Vuille et al. 2000, Garreaud and Aceituno 2001, Ronchail and Gallaire 2006, Rabatel et al. 2013). In fact, Garreaud et al. (2003) reported a significant moderate correlation ($r = -0.46$) between austral summer precipitation and the Ocean Niño Index (ONI) over the entire Altiplano, which this study similarly found between MEI and wet season precipitation over the study area ($r = -0.456$, $p < 0.01$) (Fig. 7c and Table 6). Studies (e.g., Garreaud 1999, Vuille 1999, and Garreaud et al. 2003) also found that ENSO-precipitation relationships are stronger in the western Altiplano, resulting in El Niño years with greater negative anomalies and La Niña years with greater positive anomalies. Similarly, Groups 3, 4, and 5, which occupy the western and central parts of the study region, also showed significant positive precipitation anomalies in total seasonal precipitation during La Niña events when compared with El Niño events (Figs. 3c, 3d, and 3e and Table 2).

Furthermore, significant inverse relationships between MEI and precipitation became stronger from east to west (from Groups 3 to 5) (Fig. 7 and Table 6). Plots of daily mean precipitation for these groups show anomalously positive precipitation in January and February during La Niña years (Fig. 5).

The traditional ENSO-precipitation relationship is reversed in Groups 1 and 2 in the east of the study region encompassing La Paz, most of Lake Titicaca, Cusco, and the NE half of the north central Altiplano. Though not statistically significant, these groups had on average negative seasonal and yearly total precipitation anomalies during La Niña events and positive precipitation anomalies during El Niño events. ENSO Neutral years had the largest positive precipitation anomalies out of all the ENSO phases. Seasonal precipitation anomalies were significantly greater ($p < 0.1$) during ENSO Neutral years when compared with La Niña years (Figs. 3a and 3b). In Group 3, ENSO Neutral years also produced more annual and seasonal precipitation than El Niño years, and though not statistically significant, produced positive precipitation anomalies during La Niña years as well. Analysis of daily mean precipitation during each ENSO phase reveals above average precipitation during ENSO Neutral years particularly in January (Fig. 5).

The importance of ENSO Neutral years and the diminished ENSO signal in Groups 1 and 2 still align with the limited studies (e.g. Vuille et al. 2000, Garreaud et al. 2003, Perry et al. 2017) segregating the eastern half of the study region. Eastern areas are largely characterized as having a weak response to ENSO and with no relationship between precipitation and ENSO phase (Vuille et al 2000, Garreaud et al. 2003). La Paz, for example, experienced negative precipitation anomalies from 1979-2009 for both strong El Niño and strong La Niña years (Perry et al. 2017). The authors found no studies, however, that tested the differences between ENSO Neutral years and La Niña or El Niño years in areas similar to Groups 1 and 2. This void might explain why the significant positive precipitation anomalies during ENSO Neutral years in Groups 1 and 2 have largely been unreported.

East-West Shift in Precipitation Responses to ENSO

Differences between Groups 1 and 2 with Groups 3, 4, and 5 reveal an east-west ENSO-precipitation dipole that runs along a NW – SE line roughly parallel to the southern border of Lake Titicaca. Because of their similar responses to varying ENSO phases, Groups 1 and 2 will hereafter be referenced as the eastern groups and Groups 3, 4, and 5 as the western groups. One explanation for this divide may lie in differences in moisture availability and transport to these groups during different ENSO phases. Throughout sites in the Altiplano, pluvial episodes occur when mixing ratios exceed 5 g kg^{-1} and dry episodes occur when below 3 g kg^{-1} (Garreaud et al. 2003). When mixing ratios do exceed 5 g kg^{-1}, deep convection almost invariably results (Garreaud et al. 2003).

In general, moisture advects into the Altiplano and its surrounding area from the east. Important differences in moisture transport, though, have been found outside the Altiplano in the eastern groups (Vimeux et al. 2005, Perry et al. 2017, Endries et al. 2018). While easterly moist flow still occurred in these groups, 60-70% of precipitation events originated from the north and west near Cusco and La Paz (Perry et al. 2017). Furthermore, 83% of 72-hour backward moisture trajectories from 2004 to 2010 in Cusco originated under weak flow regimes from the NW, NE, and E (Perry et al. 2014). The geomorphic configuration of the eastern groups helps explain how northwesterly flow can still provide Amazonian moisture from the northwest since moist continental lowland lies not only to the east and north but to the northwest of areas around Cusco (Fig. 1). Northwesterly oriented valleys which cut across the Andes channel moisture to the region in connection with the SALLJ (Junquas et al. 2018). For western groups, flow from the northwest would immediately advect from other mountainous regions rather than from the moist continental lowlands (Fig. 1).

Differences in moist flow also were noted during varying ENSO phases. The 2007-08 La Niña had increased moisture advection from the E and NE in Cusco while the 2009-10 El Niño had increased moisture advection from the NW and NNW (Perry et al. 2014). Those findings are consistent with increases in upper and lower level easterlies during La Niña and westerlies during El Niño (Garreaud and Aceituno 2001). Fluctuations in northwesterly flow during El Niño and La Niña, then, may explain the negative and positive precipitation anomalies. Backward trajectories during all ENSO phases in the western groups, however, should be performed for multiple years to test this hypothesis.

Scatterplots of wet season precipitation in the East and January-February MEI values reveal that positive precipitation anomalies not only appear to be more favorable in ENSO Neutral years, but weak El Niño years as well (Fig. 6). Further backward trajectory analyses in eastern groups during specific ENSO phases, including ENSO Neutral, might provide a link as to why weaker ENSO phases favor precipitation in the East. One hypothesis – that weaker flow associated with weaker ENSO phases might allow moisture to persist longer in the East – still needs to be tested. Such work to test differences in moisture availability could be done through reanalysis data but was outside the scope of this investigation.

Wet Days and Very Wet Days

The more western groups, which may receive the least moisture during El Niño years, recorded fewer wet days (approximately 16 fewer days collectively on average) during El Niño years than during La Niña years (Table 3). The eastern groups, in contrast, showed inconsistent if any changes in the number of wet days during ENSO Neutral years when proposed to receive greatest moisture availability. Specifically, when compared with La Niña, ENSO Neutral exhibited an increase of 7.3 days in Group 1 and a decrease of 1.2 days in Group 2 even though wet season precipitation during that phase increased by approximately 80 mm in both groups. Small changes (at most 1.5 days) in very wet days were reported in all groups among all ENSO phases.

The hypotheses that moisture availability varies substantially in the east and west of the study region during the same ENSO phase could also explain the differences in wet days and very wet days among the western groups. Increases in moist flow inferred from increases in mean easterly flow in the study area during DJF from 1986-1995 resulted in an increase in the number of wet days (Garreaud and Aceituno 2001). Garreaud and Aceituno (2001) used a 9-day moving average, however, eliminating short-lived episodes that may have eliminated intense events and the ability to detect an increase in intensity of precipitation with increased moist flow. Other factors or mechanisms other than moisture availability may be behind the small changes in frequency of wet day in the East but fall outside the scope of this paper.

Wet Season Onset, Dry Season Onset, and Length

Wet Season onset is earliest in the northeastern areas of the study region with Groups 1 and 2 having the earliest onsets. Groups to the southwest have wet season onsets that are progressively later in the year. The spatial relationship of wet season onset mirrors the primary direction of moisture delivery from the Amazon (Fig. 1 and Table 4) (Garreaud 1999, Perry et al. 2014). During all ENSO phases, moisture to begin the wet season is first delivered to the eastern Groups, on average around the beginning of November. As increased moisture influx occurs in the east, additional moisture advects further south and west entering the western groups. Because moisture in Group 5 would need to first pass through all the other groups, Group 5 has the latest wet season onset (1 January). Unlike the wet season onset, the dry season onset occurs within a 15-day period during all ENSO phases for all five groups. The similarity in these dates suggests regional upper-level subsidence and or a marked decrease in regional moisture influx. While Group 5 does have the earliest dry season onset, there was no discernible progression in dry season onset in the station groups as there was with wet season onset. Because wet season onset is earliest in Groups 1 and 2 and dry season onset is similar in all the groups, wet season length is also longest in Groups 1 and 2 (Fig. 4).

All groups had on average the earliest wet season onset during El Niño years out of all ENSO phases, although this was only statistically significant in Groups 1 and 2 when compared with La Niña years (Fig. 4). This finding departs from studies (e.g. Francou et al. 2003) that reference Wagnon et al. (2001) in order to support a delay in the wet season onset during El Niño years. Wagnon et al. (2001) reported through their observations of increased glacial ablation during the 1997-98 El Niño year that El Niño years associate with more dry periods throughout the wet season, not necessarily at the beginning of the wet season. The increased glacial ablation observed during El Niño might be explained by other mechanisms, such as increased temperature (Bradley et al. 2006, Ramirez et al. 2001), decreased albedo

(Francou et al. 2003), an increased fraction of precipitation falling as rain (Endries et al. 2018), or larger spans of sunny days during the wet season (Francou et al. 2003, Favier et al. 2004). Evaluation of these mechanisms, however, is outside the scope of this study.

ENSO Flavors and Other Limitations

Analysis of the scatterplots of wet season precipitation and January-February MEI values reveals that ENSO events of comparable magnitude do not evoke the same response (Fig. 6). For instance, wet season totals in Group 4 vary over 400 mm among the four strongest El Niño events, with totals in the El Niño of 1997-98 comparable to the four strongest La Niña events. Indeed, Sulca et al. (2017) found varying precipitation responses in southern Peru depending if warmer waters were centered over the Central Tropical Pacific or the Eastern Tropical Pacific.

Whereas ENSO phases are forecast months in advance (Climate Prediction Center), the MEI and this study do not distinguish among differing SST patterns in different Pacific Ocean regions which limits accurate predictions of precipitation responses to ENSO phases in the western groups. Prediction of precipitation responses by ENSO phase in the eastern groups, however, may be more accurate regardless of which type of ENSO persists. The scatterplots in Group 1 and 2 reveal tighter groups of wet season totals among the strongest El Niño and La Niña years.

This study also did not test relationships with other teleconnection patterns or forcings that may also exert some degree of control in precipitation variability in the study area. Veettil et al. (2016) demonstrated that when the warm phase of PDO and El Niño or the cold phase of PDO and La Niña align, the response in glacial mass balance is amplified in southern Peru and Bolivia. By only looking at ENSO, this study possibly misses key components to understanding and predicting precipitation variability.

Finally, the authors acknowledge that station coverage reporting consistent precipitation observations was limited. The filtering method applied eliminated about 90% of the total stations in the database which produced a large observational gap south and west of Cusco. Unfortunately, lowering completeness thresholds to as low as 70% from 1972-2016 still did not fill this gap. While grouping analyses were done on the two clusters of stations within Group 1 to verify that they both independently would form a separate group, the lack of coverage ultimately made delineation of boundaries between group domains impossible. Mortensen et al. (2018) offer a plausible solution to increase station density by interpolating missing data using multiple regressions based on existing monthly statistics from highly correlated nearby stations. Since no infilling was performed, findings from this analysis could help validate future work employing this method.

6. Summary and Conclusions

This paper has improved the understanding of ENSO-precipitation relationships in the outer tropical Andes of southern Peru and Bolivia. By creating five optimally chosen station groups in the outer tropical Andes of southern Peru and Bolivia, this study uncovered two areas (East and West) with differing precipitation responses to ENSO forcing of regional climate. The western groups (Groups 3, 4, and 5), farthest from the Amazon, largely followed the traditional understanding of ENSO-precipitation relationships producing fewer wet days, fewer very wet days, negative annual precipitation anomalies, and negative seasonal precipitation anomalies during El Niño years than in with La Niña years. The eastern groups, nearest to the Amazon and incorporating sites such as Quelccaya Icecap, Cusco, and La Paz, exhibit the highest wet season and annual precipitation during ENSO Neutral years of all ENSO classes. Additionally, during El Niño, these groups produced more wet days, more very wet days, positive annual precipitation anomalies, and positive seasonal precipitation anomalies than in La Niña years, although none of these variables are statistically different. Finally, although some studies (e.g., Francou et al. 2003) suggested wet season onset was delayed during El Niño when compared with ENSO Neutral or La Niña years, this paper demonstrated wet season onset was earliest during El Niño years and was most delayed during La Niña years in all five station groups.

Together these findings can now be used to better interpret ENSO predictions for their sub-regional outcomes across the northern Altiplano and surrounding areas in southern Peru and Bolivia. El Niño years and La Niña years produce deficits and increases in precipitation, respectively, in the West, while in the East both phases produce deficits with ENSO Neutral years producing the largest positive precipitation anomalies. Reinterpretation of ice cores from glaciers such as Quelccaya Icecap located in the East may be necessary, as these findings may suggest more annual accumulation during ENSO Neutral years.

The distinct ENSO-precipitation dipole across the study region may relate to different moisture transport and availability characteristics according to ENSO phase. ENSO Neutral years may favor moisture availability in the East through weak flow which allows moisture to persist in that area while El Niño years favor increased northwesterly flow (Perry et al. 2014), resulting in less moisture availability in the West due to the geomorphic configuration of that area. Such hypotheses in moisture transport could be tested throughout the study region by employing methods such as computing backward trajectories of precipitating events. The inclusion of ENSO Neutral years as its own class in future analyses of ENSO-precipitation relationships is also essential. Additionally, the findings on early wet season onset during El Niño events should be further tested and correlated with the start of the agricultural season so that the information can serve stakeholders in the region.

7. Acknowledgements

The authors are grateful for the dedicated professionals of SENAMHI Peru, SENAMHI Bolivia, the DECADE Project, and the ESRL of NOAA for the countless hours of work necessary to observe, formulate, and make available the critical climate data for this paper. This work is supported by funding from the National Science Foundation Grant AGS-1347179 (CAREER: Multiscale Investigations of Tropical Andean Precipitation) to L.B. Perry. Special thanks are also due to Dr. Johnathan Sugg and Montana Eck for invaluable advice and feedback, and to partners and other family members for their patience and loving support.

References

Aalto, R., Maurice-Bourgoin, L., Dunne, T., Montgomery, D.R., Nittrouer, C.A. and Guyot, J.L., 2003. Episodic sediment accumulation on Amazonian flood plains influenced by El Nino/Southern Oscillation. Nature, 425(6957), p.493.

Aceituno, P., 1988. On the functioning of the Southern Oscillation in the South American sector. Part I: Surface climate. Monthly Weather Review, 116(3), pp.505-524.

Anderson, E.P., Marengo, J., Villalba, R., Halloy, S., Young, B., Cordero, D., Gast, F., Jaimes, E., Ruiz, D., Herzog, S.K. and Martinez, R., 2017. Consequences of climate change for ecosystems and ecosystem services in the tropical Andes.

Andrade, M.F., Moreno, I., Calle, J.M., Ticona, L., Blacutt, L., Lavado-Casimiro, W., Sabino, E., Huerta, A., Aybar, C., Hunziker, S. and Brönnimann, S., 2018. Atlas-Clima y eventos extremos del Altiplano Central perú-boliviano.

Bonferroni, C., 1936. Teoria statistica delle classi e calcolo delle probabilita. Pubblicazioni del R Istituto Superiore di Scienze Economiche e Commericiali di Firenze, 8, pp.3-62.

Bradley, R.S., Vuille, M., Diaz, H.F. and Vergara, W., 2006. Threats to water supplies in the tropical Andes. Science, 312(5781), pp.1755-1756.

Caliński, T. and Harabasz, J., 1974. A dendrite method for cluster analysis. Communications in Statistics-theory and Methods, 3(1), pp.1-27.

Chavez, S.P. and Takahashi, K., 2017. Orographic rainfall hot spots in the Andes-Amazon transition according to the TRMM precipitation radar and in situ data. Journal of Geophysical Research: Atmospheres, 122(11), pp.5870-5882.

Climate Prediction Center, 2018. Climate Prediction Center - ONI. [online] Origin.cpc.ncep.noaa.gov. Available at: http://origin.cpc.ncep.noaa.gov/products/analysis_monitoring/ensostuff/ONI_v5.php [Accessed 15 Nov. 2018].

DECADE, 2018. DECADE. [online] Institute of Geography, U. Bern. Available at: http://www.geography.unibe.ch/research/climatology_group/research_projects/decade/index_eng.html [Accessed 22 Oct. 2018].

Dunn, O.J., 1964. Multiple comparisons using rank sums. Technometrics, 6(3), pp.241-252.

Earth System Research Lab, 2018. ESRL : PSD : Multivariate ENSO Index (MEI). [online] Esrl.noaa.gov. Available at: https://www.esrl.noaa.gov/psd/enso/mei/ [Accessed 22 Oct. 2018].

Eck, M.A., Perry, L.B., Soulé, P.T., Sugg, J.W. and Miller, D.K., 2017. Winter climate variability in the southern Appalachian Mountains, 1910–2017. International Journal of Climatology.

Endries, J.L., Perry, L.B., Yuter, S.E., Seimon, A., Andrade-Flores, M., Winkelmann, R., Quispe, N., Rado, M., Montoya, N., Velarde, F. and Arias, S., 2018. Radar-Observed Characteristics of Precipitation in the Tropical High Andes of Southern Peru and Bolivia. Journal of Applied Meteorology and Climatology, (2018).

Espinoza, J.C., Chavez, S., Ronchail, J., Junquas, C., Takahashi, K. and Lavado, W., 2015. Rainfall hotspots over the southern tropical Andes: Spatial distribution, rainfall intensity, and relations with large-scale atmospheric circulation. Water Resources Research, 51(5), pp.3459-3475.

Favier, V., Wagnon, P. and Ribstein, P., 2004. Glaciers of the outer and inner tropics: A different behaviour but a common response to climatic forcing. Geophysical Research Letters, 31(16).

Figueroa, S.N., Satyamurty, P. and Da Silva Dias, P.L., 1995. Simulations of the summer circulation over the South American region with an eta coordinate model. Journal of the atmospheric sciences, 52(10), pp.1573-1584.

Francou, B. and Pizarro, L., 1985. EL NINO Y LA SEQUÍA EN LOS ALTOS ANDES CENTRALES. Bull. Inst. Fr. Et. And, 14(1-2), pp.1-18.

Francou, B., Vuille, M., Wagnon, P., Mendoza, J. and Sicart, J.E., 2003. Tropical climate change recorded by a glacier in the central Andes during the last decades of the twentieth century: Chacaltaya, Bolivia, 16 S. Journal of Geophysical Research: Atmospheres, 108(D5).

Francou, B., and Vincent, C., 2007. "Les glaciers à l'épreuve du climat" Paris: Editions Belin-IRD, p. 274

Garreaud, R., 1999. Cold air incursions over subtropical and tropical South America: A numerical case study. Monthly Weather Review, 127(12), pp.2823-2853.

Garreaud, R., 2000. Cold air incursions over subtropical South America: Mean structure and dynamics. Monthly Weather Review, 128(7), pp.2544-2559.

Garreaud, R. and Aceituno, P., 2001. Interannual rainfall variability over the South American Altiplano. Journal of Climate, 14(12), pp.2779-2789.

Garreaud, R., Vuille, M. and Clement, A.C., 2003. The climate of the Altiplano: observed current conditions and mechanisms of past changes. Palaeogeography, palaeoclimatology, palaeoecology, 194(1-3), pp.5-22.

Graham, N.E., 1994. Decadal-scale climate variability in the tropical and North Pacific during the 1970s and 1980s: Observations and model results. Climate Dynamics, 10(3), pp.135-162.

Guy, H., Seimon, A., Perry, L. B., Konecky, B., Rado, M., Andrade, M., Potocki, M., Mayewski, P., 2018. Subseasonal variations of stable isotopes in tropical Andean precipitation. Journal of Hydrometeorology, in review.

Haines, S.A., Mayewski, P.A., Kurbatov, A.V., Maasch, K.A., Sneed, S.B., Spaulding, N.E., Dixon, D.A. and Bohleber, P.D., 2016. Ultra-high resolution snapshots of three multi-decadal periods in an Antarctic ice core. Journal of Glaciology, 62(231), pp.31-36.

Hartigan, J.A. and Wong, M.A., 1979. Algorithm AS 136: A k-means clustering algorithm. Journal of the Royal Statistical Society. Series C (Applied Statistics), 28(1), pp.100-108.

Hunziker, S., Brönnimann, S., Calle, J., Moreno, I., Andrade, M., Ticona, L., Huerta, A. and Lavado-Casimiro, W., 2018. Effects of undetected data quality issues on climatological analyses. Climate of the Past, 14(1), pp.1-20.

Junquas, C., Takahashi, K., Condom, T., Espinoza, J.C., Chavez, S., Sicart, J.E. and Lebel, T., 2018. Understanding the influence of orography on the precipitation diurnal cycle and the associated atmospheric processes in the central Andes. Climate dynamics, 50(11-12), pp.3995-4017.

Knüsel, S., Brütsch, S., Henderson, K.A., Palmer, A.S. and Schwikowski, M., 2005. ENSO signals of the twentieth century in an ice core from Nevado Illimani, Bolivia. Journal of Geophysical Research: Atmospheres, 110(D1).

Kruskal, W.H. and Wallis, W.A., 1952. Use of ranks in one-criterion variance analysis. Journal of the American statistical Association, 47(260), pp.583-621.

Liebmann, B., Camargo, S.J., Seth, A., Marengo, J.A., Carvalho, L.M., Allured, D., Fu, R. and Vera, C.S., 2007. Onset and end of the rainy season in South America in observations and the ECHAM 4.5 atmospheric general circulation model. Journal of Climate, 20(10), pp.2037-2050.

Mantua, N.J. and Hare, S.R., 2002. The Pacific decadal oscillation. Journal of oceanography, 58(1), pp.35-44.

Mortensen, E., Wu, S., Notaro, M., Vavrus, S., Montgomery, R., De Piérola, J., Sánchez, C. and Block, P., 2018. Regression-based season-ahead drought prediction for southern Peru conditioned on large-scale climate variables. Hydrology and Earth System Sciences, 22(1), p.287.

Nitta, T. and Yamada, S., 1989. Recent warming of tropical sea surface temperature and its relationship to the Northern Hemisphere circulation. Journal of the Meteorological Society of Japan. Ser. II, 67(3), pp.375-383.

Perry, L.B., Seimon, A. and Kelly, G.M., 2014. Precipitation delivery in the tropical high Andes of southern Peru: new findings and paleoclimatic implications. International Journal of Climatology, 34(1), pp.197-215.

Perry, L.B., Seimon, A., Andrade-Flores, M.F., Endries, J.L., Yuter, S.E., Velarde, F., Arias, S., Bonshoms, M., Burton, E.J., Winkelmann, I.R. and Cooper, C.M., 2017. Characteristics of precipitating storms in glacierized tropical Andean cordilleras of Peru and Bolivia. Annals of the American Association of Geographers, 107(2), pp.309-322.

Philander, S.G.H., 1983. El Nino southern oscillation phenomena. Nature, 302(5906), p.295.

Rabatel, A., Francou, B., Soruco, A., Gomez, J., Cáceres, B., Ceballos, J.L., Basantes, R., Vuille, M., Sicart, J.E., Huggel, C. and Scheel, M., 2012. Current state of glaciers in the tropical Andes: a multi-century perspective on glacier evolution and climate change. The Cryosphere, 7(1), pp.81-102.

Ramirez, E., Francou, B., Ribstein, P., Descloitres, M., Guerin, R., Mendoza, J., Gallaire, R., Pouyaud, B. and Jordan, E., 2001. Small glaciers disappearing in the tropical Andes: a case-study in Bolivia: Glaciar Chacaltaya (16 o S). Journal of Glaciology, 47(157), pp.187-194.

Ramirez, E., Hoffmann, G., Taupin, J.D., Francou, B., Ribstein, P., Caillon, N., Ferron, F.A., Landais, A., Petit, J.R., Pouyaud, B. and Schotterer, U., 2003. A new Andean deep ice core from Nevado Illimani (6350 m), Bolivia. Earth and Planetary Science Letters, 212(3-4), pp.337-350.

Ribstein, P., Tiriau, E., Francou, B. and Saravia, R., 1995. Tropical climate and glacier hydrology: a case study in Bolivia. Journal of Hydrology, 165(1-4), pp.221-234.

Rodwell, M.J. and Hoskins, B.J., 2001. Subtropical anticyclones and summer monsoons. Journal of Climate, 14(15), pp.3192-3211.

Ronchail, J. and Gallaire, R., 2006. ENSO and rainfall along the Zongo valley (Bolivia) from the Altiplano to the Amazon basin. International Journal of Climatology: A Journal of the Royal Meteorological Society, 26(9), pp.1223-1236.

Seluchi, M.E., Saulo, A.C., Nicolini, M. and Satyamurty, P., 2003. The northwestern Argentinean low: A study of two typical events. Monthly Weather Review, 131(10), pp.2361-2378.

SENAMHI Bolivia, 2018. SENAMHI - Página principal. [online] Senamhi.gob.bo. Available at: http://senamhi.gob.bo/index.php/inicio [Accessed 22 Oct. 2018].

SENAMHI Peru, 2018. SENAMHI - Perú. [online] Senamhi.gob.pe. Available at: https://www.senamhi.gob.pe/ [Accessed 22 Oct. 2018].

Sicart, J.E., Hock, R., Ribstein, P., Litt, M. and Ramirez, E., 2011. Analysis of seasonal variations in mass balance and meltwater discharge of the tropical Zongo Glacier by application of a distributed energy balance model. Journal of Geophysical Research: Atmospheres, 116(D13).

Skamarock, W.C. and Klemp, J.B., 2008. A time-split nonhydrostatic atmospheric model for weather research and forecasting applications. Journal of Computational Physics, 227(7), pp.3465-3485.

Soruco, A., Vincent, C., Francou, B. and Gonzalez, J.F., 2009. Glacier decline between 1963 and 2006 in the Cordillera Real, Bolivia. Geophysical Research Letters, 36(3).

Sulca, J., Takahashi, K., Espinoza, J.C., Vuille, M. and Lavado-Casimiro, W., 2018. Impacts of different ENSO flavors and tropical Pacific convection variability (ITCZ, SPCZ) on austral summer rainfall in South America, with a focus on Peru. International Journal of Climatology, 38(1), pp.420-435.

Thompson, L.G., Mosley-Thompson, E., Dansgaard, W. and Grootes, P.M., 1986. The Little Ice Age as recorded in the stratigraphy of the tropical Quelccaya ice cap. Science, 234(4774), pp.361-364.

Trenberth, K.E., 1997. The definition of el nino. Bulletin of the American Meteorological Society, 78(12), pp.2771-2778.

Urrutia, R. and Vuille, M., 2009. Climate change projections for the tropical Andes using a regional climate model: Temperature and precipitation simulations for the end of the 21st century. Journal of Geophysical Research: Atmospheres, 114(D2).

Veettil, B.K., Bremer, U.F., de Souza, S.F., Maier, É.L.B. and Simões, J.C., 2016. Influence of ENSO and PDO on mountain glaciers in the outer tropics: case studies in Bolivia. Theoretical and applied climatology, 125(3-4), pp.757-768.

Vimeux, F., Gallaire, R., Bony, S., Hoffmann, G. and Chiang, J.C., 2005. What are the climate controls on δD in precipitation in the Zongo Valley (Bolivia)? Implications for the Illimani ice core interpretation. Earth and Planetary Science Letters, 240(2), pp.205-220.

Vuille, M., Hardy, D.R., Braun, C., Keimig, F. and Bradley, R.S., 1998. Atmospheric circulation anomalies associated with 1996/1997 summer precipitation events on Sajama Ice Cap, Bolivia. Journal of Geophysical Research: Atmospheres, 103(D10), pp.11191-11204.

Vuille, M., 1999. Atmospheric circulation over the Bolivian Altiplano during dry and wet periods and extreme phases of the Southern Oscillation. International Journal of Climatology, 19(14), pp.1579-1600.

Vuille, M., Bradley, R.S. and Keimig, F., 2000. Interannual climate variability in the Central Andes and its relation to tropical Pacific and Atlantic forcing. Journal of Geophysical Research: Atmospheres, 105(D10), pp.12447-12460.

Vuille, M., Carey, M., Huggel, C., Buytaert, W., Rabatel, A., Jacobsen, D., Soruco, A., Villacis, M., Yarleque, C., Timm, O.E. and Condom, T., 2017. Rapid decline of snow and ice in the tropical Andes–Impacts, uncertainties and challenges ahead. Earth-Science Reviews.

Wagnon, P., Ribstein, P., Francou, B. and Sicart, J.E., 2001. Anomalous heat and mass budget of Glaciar Zongo, Bolivia, during the 1997/98 El Nino year. Journal of Glaciology, 47(156), pp.21-28.

Table 1. Summary of data sets used.

Data Type	Temporal Resolution	Period	Source
1. **Precipitation**			
SENAMHI sites of Bolivia (533)	Daily	1972 – 2017	DECADE Project and SENAMHI Bolivia
SENAMHI sites of Peru (241)	Daily	1972 – 2018	SENAMHI Peru
2. **Teleconnection Pattern Indices**			
Multivariate ENSO Index (MEI)	Monthly	1871 – 2018	U.S. Earth System Research Lab, NOAA

Table 2. Average total wet season precipitation (mm) of all observation stations within the entire study region (All) and within Groups 1-5 averaged over the hydrological years from 1972-2016 (Mean) and averaged over only El Niño, La Niña, and ENSO Neutral years from that same period. Differences between La Niña (LN), El Niño (EN), and ENSO Neutral years (NE) are also reported.

Group	Mean	El Niño	La Niña	Neutral	LN-EN Diff	NE-LN Diff	EN-NE Diff
1	569	564	524	601	-40	77	-37
2	516	497	477	559	-20	82	-62
3	500	447	528	541	81	13	-94
4	398	341	476	413	135	-63	-72
5	219	169	302	224	133	-78	-55
All	450	414	464	480	50	16	-66

Table 3. Average number of wet days of all observation stations within the entire study region (All) and within Groups 1-5 averaged over the hydrological years from 1972-2016 (Mean) and averaged over only El Niño, La Niña, and ENSO Neutral years from that same period. Differences between La Niña (LN), El Niño (EN), and ENSO Neutral years (NE) are also reported.

Group	Mean	El Niño	La Niña	Neutral	LN-EN Diff	NE-LN Diff	EN-NE Diff
1	110.5	110.1	111.6	110.4	1.5	-1.2	-0.3
2	107.2	103.1	105.4	112.7	2.3	7.3	-9.5
3	95.7	90.7	98.4	99.4	7.7	1.0	-8.7
4	77.0	69.2	86.9	79.4	17.6	-7.4	-10.2
5	44.3	36.1	58.0	44.9	21.9	-13.0	-8.8
All	88.7	83.7	93.1	91.5	9.4	-1.6	-7.7

Table 4. Average wet season onset (month/day) of all observation stations within the entire study region (All) and within Groups 1-5 averaged over the hydrological years from 1972-2016 (Mean) and averaged over only El Niño, La Niña, and ENSO Neutral years from that same period. Differences between La Niña (LN), El Niño (EN), and ENSO Neutral years (NE) are also reported.

Group	Mean	El Niño	La Niña	Neutral	LN-EN Diff	NE-LN Diff	EN-NE Diff
1	11/11	11/4	11/24	11/11	20	-13	-7
2	11/20	11/10	12/7	11/21	27	-16	-11
3	12/7	12/2	12/13	12/8	11	-5	-6
4	12/15	12/11	12/20	12/16	9	-4	-5
5	12/29	12/26	1/1	12/31	6	-1	-5
All	12/2	11/28	12/9	12/2	11	-7	-4

Table 5. Average wet season length (days) of all observation stations within the entire study region (All) and within Groups 1-5 averaged over the hydrological years from 1972-2016 (Mean) and averaged over only El Niño, La Niña, and ENSO Neutral years from that same period. Differences between La Niña (LN), El Niño (EN), and ENSO Neutral years (NE) are also reported.

Group	Mean	El Niño	La Niña	Neutral	LN-EN Diff	NE-LN Diff	EN-NE Diff
1	154.2	160.7	138.7	156.4	-22.0	17.7	4.3
2	139.1	146.1	120.9	142.4	-25.2	21.5	3.7
3	126.0	131.6	117.7	125.1	-13.9	7.4	6.5
4	122.8	127.9	115.0	122.1	-12.9	7.1	5.8
5	95.7	97.3	94.6	94.7	-2.7	0.1	2.6
All	130.9	134.8	122.1	131.9	-12.7	9.8	2.8

Table 6. Spearman's correlation values between annual MEI bimonthly index values and average annual precipitation characteristics within the entire study region (All) and within Groups 1-5: wet season onset, wet season length, wet season total, hydrological year total, wet days, and very wet days. Correlations significant at the 0.05 level and 0.01 level (2-tailed) are denoted with * and **, respectively.

Group	**September-October**					**January-February**			
	Wet Season Onset	Wet Season Length	Wet Season Total	Wet Days	Very Wet Days	Wet Season Total	Hydrological Year Total	Wet Days	Very Wet Days
1	**-0.448****	**0.409****	0.135	-0.096	**0.447****	-0.042	-0.075	-0.126	**0.304***
2	**-0.476****	**0.346***	0.034	-0.116	-0.008	-0.109	-0.116	-0.211	-0.134
3	-0.147	0.213	**-0.412****	-0.284	-0.248	**-0.543****	**-0.495****	**-0.391****	**-0.441****
4	-0.192	0.095	**-0.528****	**-0.427****	**-0.336***	**-0.580****	**-0.532****	**-0.484****	**-0.390****
5	-0.084	-0.050	**-0.501****	**-0.536****	**-0.334***	**-0.604****	**-0.559****	**-0.611****	**-0.448****
All	-0.204	0.230	**-0.338***	-0.289	-0.147	**-0.456****	**-0.443****	**-0.406****	-0.286

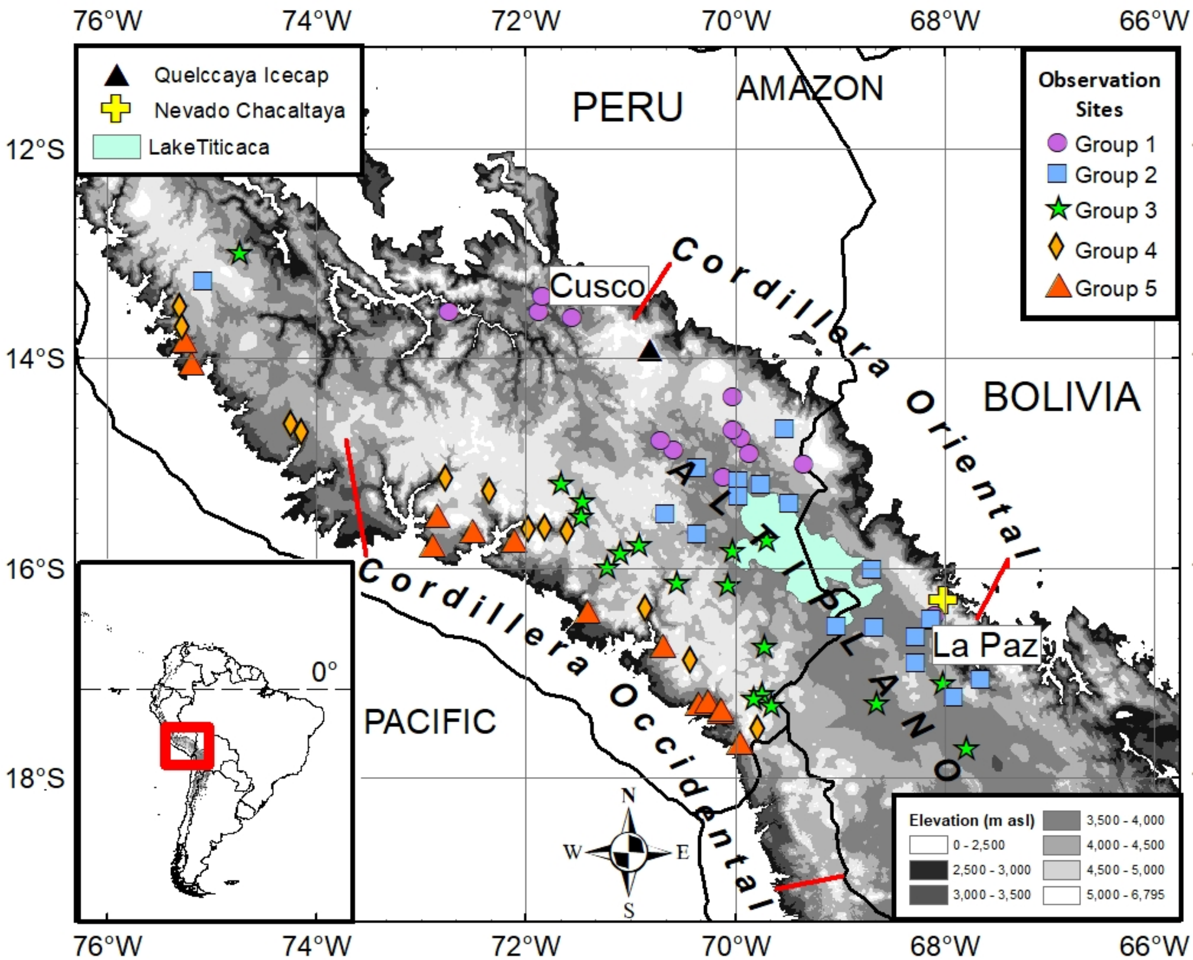

Fig. 1. Map of study region with the 75 observation sites above 2500 m that had 90% or more completeness in precipitation observations from 1972-2016. The sites were grouped into five groups by average wet season onset over 1972-2016 using the K-means grouping method in ArcMap 10.4.1.

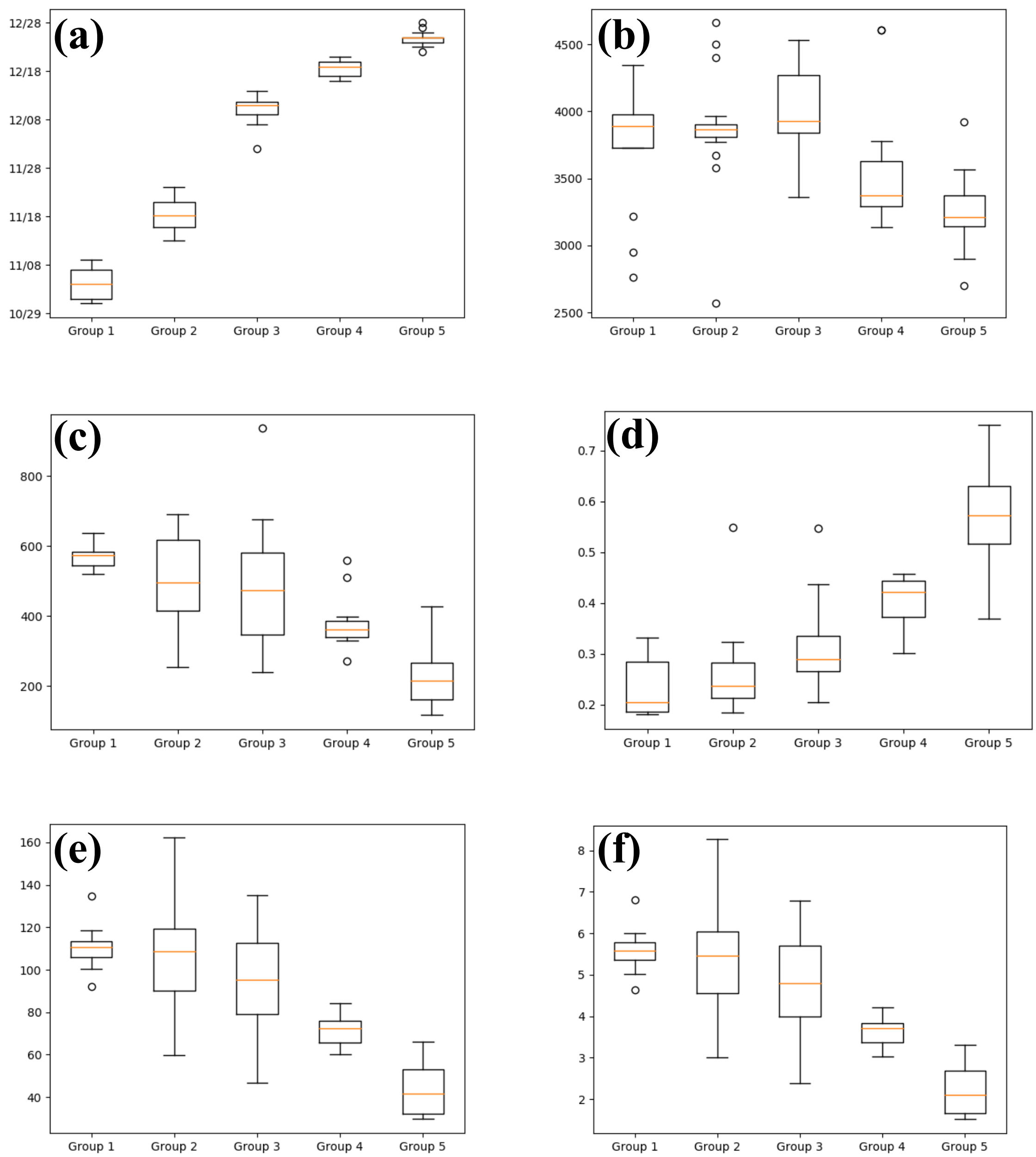

Fig. 2. Box and whisker plots displaying minimum, first quartile, median, third quartile, and maximum wet season onset (month/day) (a), elevation (m) (b), total wet season precipitation (mm) (c), coefficient of variation of total wet season precipitation (d), wet days (e), and very wet days (≥ 95th percentile) (f) of the 75 observations sites according to group.

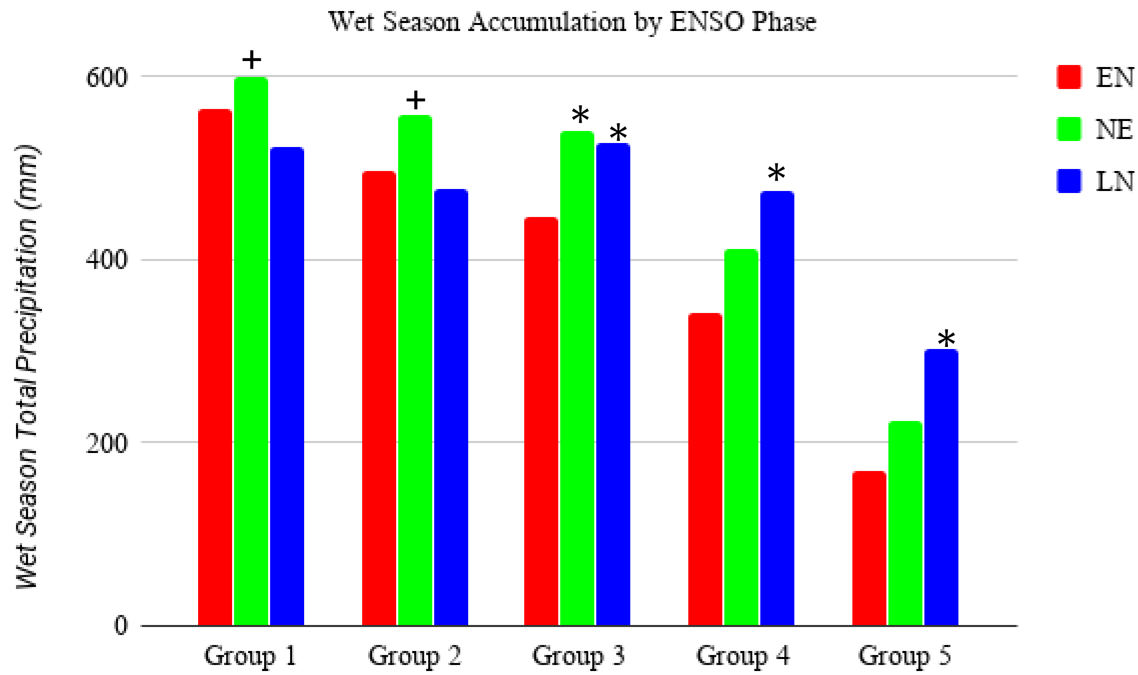

Fig. 3. Bar graph displaying wet season totals (mm) from 1972-2016 for Groups 1-5 averaged by ENSO phase: El Niño (red, n=18), ENSO Neutral (green, n=17), and La Niña (blue, n=10). ENSO phases with significantly greater wet season totals than the phase with the lowest wet season total are indicated with a '*' for p < 0.05 or '+" for p < 0.1.

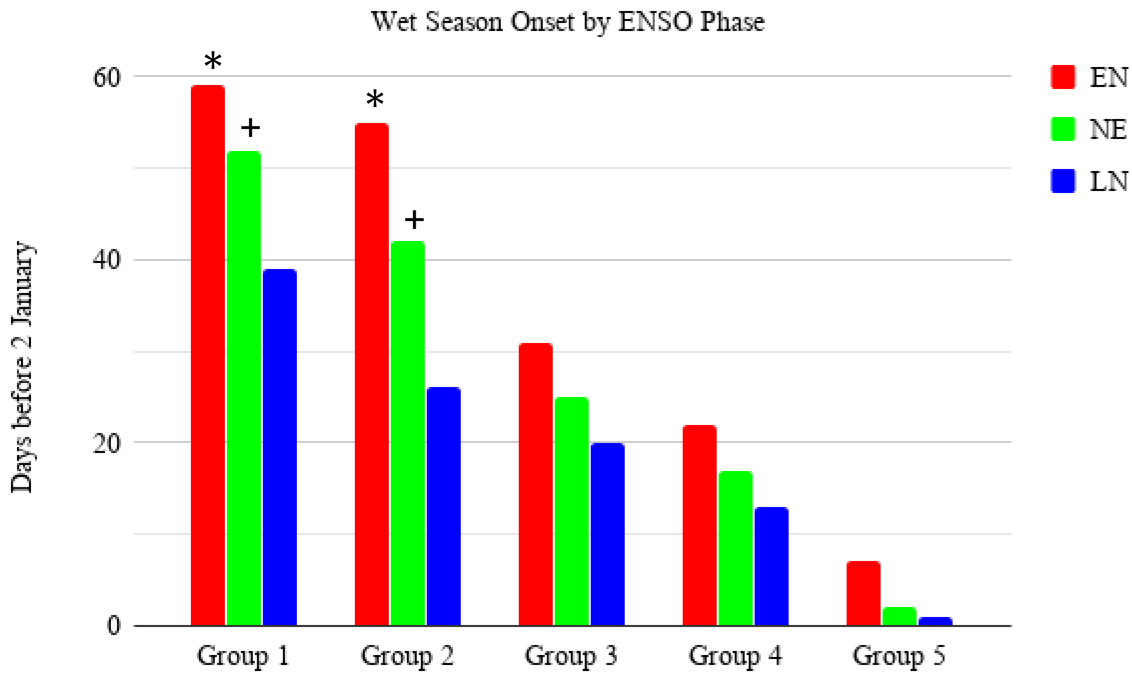

Fig. 4. Bar graph displaying days before 2 January the wet season began from 1972-2016 for Groups 1-5 averaged by ENSO phase: El Niño (red, n =18), ENSO Neutral (green, n=17), and La Niña (blue, n=10). ENSO phases with a significantly earlier wet season onset than the phase with the latest wet season onset are indicated with a '*' for $p < 0.05$ or '+" for $p < 0.1$.

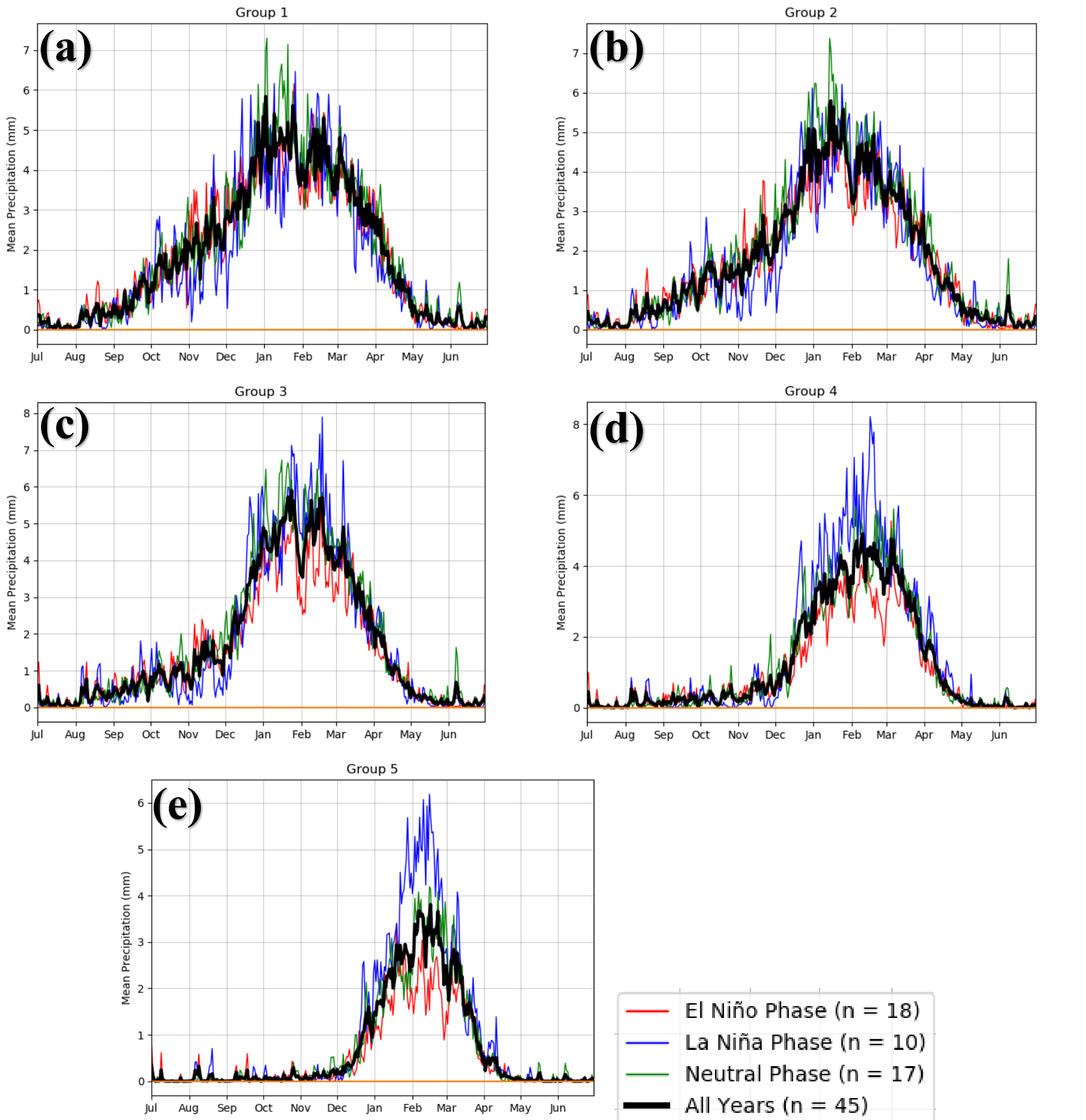

Fig. 5. Line graph displaying daily mean precipitation (mm) from 1972-2016 for Group 1 (a), Group 2 (b), Group 3 (c), Group 4 (d), and Group 5 (e) during El Niño years only (red, n=18), ENSO Neutral years only (green, n=17), La Niña years only (blue, n=10), and all years (black, n=45).

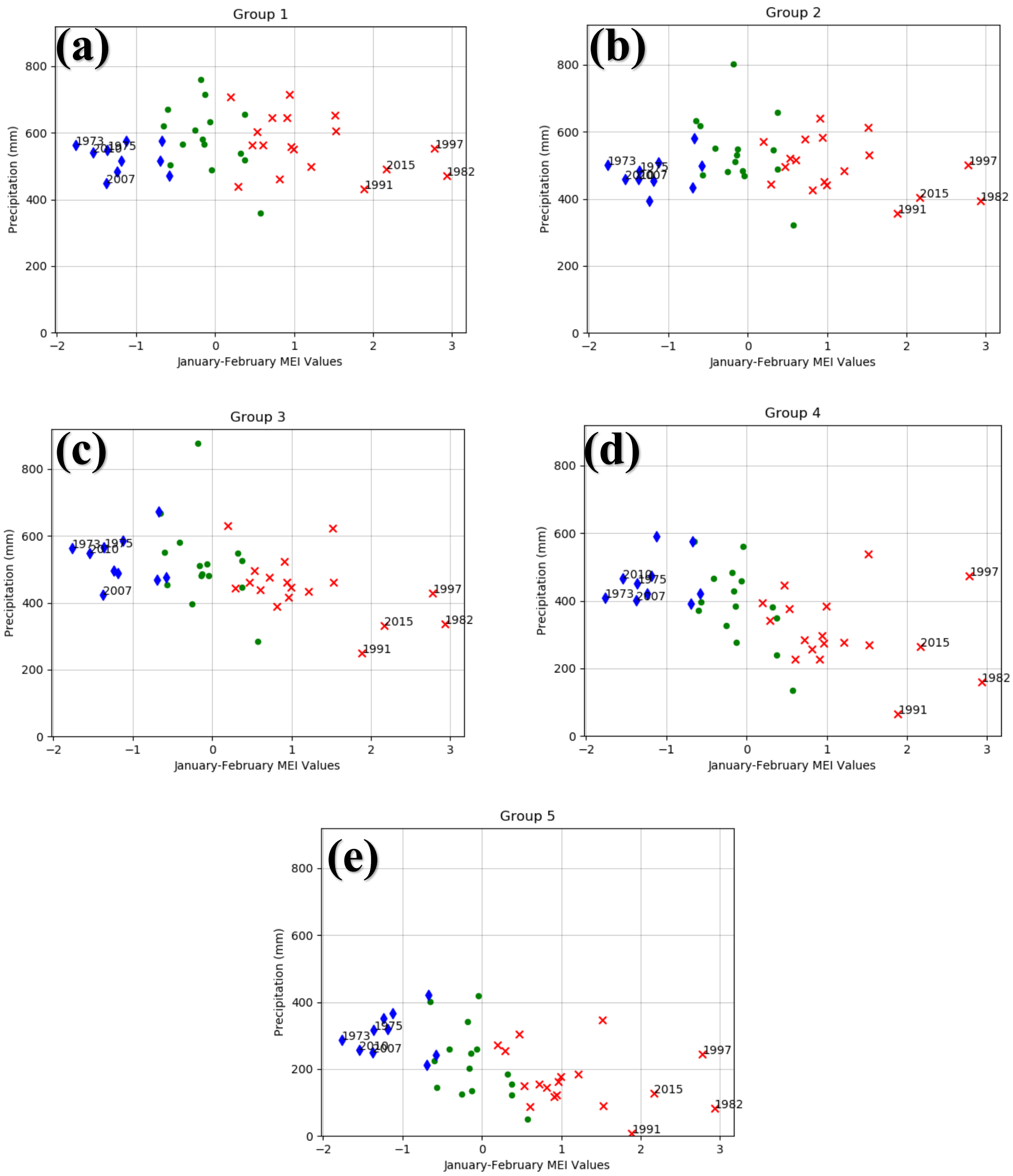

Fig. 6. Scatterplot displaying January-February MEI values and corresponding wet season total precipitation (mm) for each hydrological year from 1972-2016 for Group 1 (a), Group 2 (b), Group 3 (c), Group 4 (d), and Group 5 (e). Hydrological years classified as El Niño (red x, n=18), ENSO Neutral (green circle, n=17), and La Niña (blue diamond, n=10). The strongest four La Niña years (1973, 1975, 2007, and 2010) and El Niño years (1982, 1991, 1997, and 2015) are labeled by the hydrological year in which they occurred.

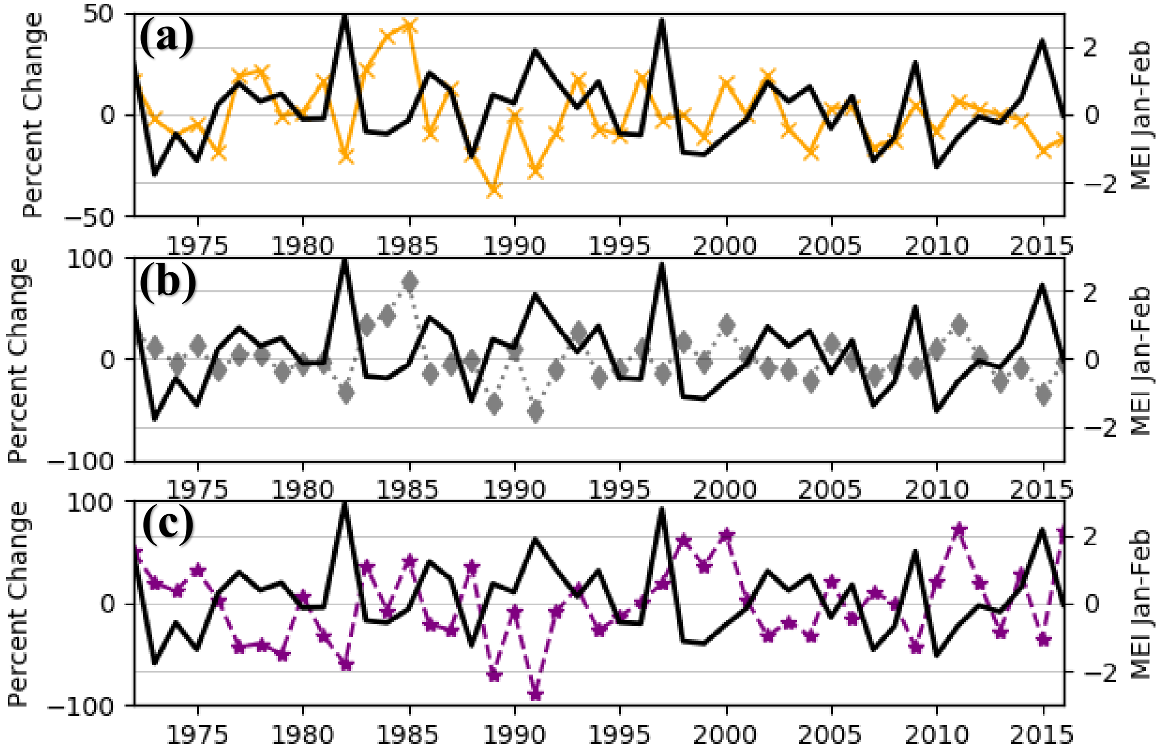

Fig. 7. Line graph displaying percent change in the wet season total from the mean wet season total from 1972-2016 for a) the average of Groups 1-2, b) Group 3, and the average of Groups 4-5. January-February MEI values are plotted in black from 1972-2016 to provide ENSO phase and strength.

Vita

Joseph Jonaitis was born and raised in Grand Rapids, Michigan, by his loving parents with his two siblings. While in Michigan, Joe formed a love of nature and an intrigue with how nature worked, including the weather. Camping, exploring in nature, playing sports, or measuring the latest snowfall or creek flood stage kept him outside the majority of his time. Joe graduated as valedictorian with a B.S. in physiology from Michigan State University and joined the Peace Corps soon after. For two and a half years, Joe served his community members in Guatemala in sustainable agriculture, health and nutrition, and medical team translations. After Guatemala, Joe worked as a federal investigator for the U.S. Department of Labor, enforcing labor laws and protecting domestic and foreign workers for over five years. Upon marrying his wife, the two left Michigan in pursuit of new service opportunities, new dreams and life directions, and time and space to build a foundation for their marriage. During this time of living and growing in new places, Joe rediscovered his passion for weather and teaching. He joined Dr. L. Baker Perry's research team while earning a master's degree in Geography at Appalachian State University. After graduation, Joe and his wife moved back to Grand Rapids with their newborn child where he began teaching at Muskegon Community College.